EUROPEAN JOURNAL OF MATERIALS SCIENCE AND ENGINEERING
Volume 10, Issue 4, 2025: 237-244 | www.ejmse.ro | ISSN: 2537-4338

EJMSE

DOI: 10.36868/ejmse.2025.10.04.237

INFLUENCE OF CELLULOSE ON THE PHYSICO-CHEMICAL CHARACTERIZATIONS OF ALKALI-ACTIVATED GEOPOLYMERS

Mouna SELLAMI[1,*] [0000-0001-9112-1155], Hebat-Allah S. TOHAMY[2] [0000-0001-5494-841X], Dumitru-Doru BURDUHOS-NERGIȘ[3] [0000-0002-2716-1328], Petrică VIZUREANU[3,4] [0000-0002-3593-9400], Andrei Victor SANDU[3,4,5,] [0000-0002-9292-749X], Mohamed TOUMI[1] [0000-0003-0406-627X]

[1] Laboratoire Physico-Chimie de L'Etat Solide, Faculté Des Sciences de Sfax, Université du Sfax, Route de Soukra Km3.5, BP 802, 3018 Sfax, Tunisia
[2] Cellulose and Paper Department, National Research Centre, 33 El Bohouth Str., P.O. 12622, Dokki, Giza, Egypt
[3] "Gheorghe Asachi" Technical University of Iasi, Faculty of Material Science and Engineering, Blvd. Dimitrie Mangeron, No. 41, 700050 Iasi, Romania
[4] Academy of Romanian Scientists, 54 Splaiul Independentei, 050094 Bucharest, Romania
[5] Romanian Inventors Forum, Str. Sf. P. Movila 3, 700089 Iasi, Romania

Abstract

Cellulose is widely recognized as a plentiful, renewable and optically active source of carbohydrate polymers. This research contributes to our understanding of the effect of incorporating cellulose into a metakaolin-based geopolymer matrix on its morphological and optical behaviour with the aim of expanding the range of applications for this eco-friendly material. The cellulose was incorporated as an additive into geopolymers with different weight percentages: 0.5%, 1%, 1.5%, and 2%. XRD diagrams of geopolymers display a broad amorphous hump, confirming the polymeric character of samples, with noticeable peaks correlated to illite, quartz, SiO_2, and cellulose crystalline phases. The results obtained were confirmed by FTIR spectroscopy. The morphology of the samples was investigated by SEM, and the results indicate that the optimal concentrations of cellulose are 0.5 and 1 wt%. UV-VIS analysis revealed a significant increase in absorbance in the UV and visible regions of the G2 spectrum, corresponding to the highest amount of cellulose incorporated.

Keywords: *alkali-activated geopolymers, cellulose, UV-VIS absorbance, SEM analysis*

Introduction

Geopolymers, also known as inorganic polymers, are materials formed by chemically activating aluminosilicate sources (minerals rich in aluminum and silicon, such as metakaolin, slag, and fly ash) [1-2]. Due to their dielectric performance, mechanical strength, chemical resistance, and low carbon footprint, geopolymers are being increasingly studied for applications in civil engineering, refractory materials, hazardous waste immobilization, and advanced composites [3-6].

Despite these advantages, geopolymers display low fracture toughness (resistance to crack propagation) and are prone to microcracking (formation of tiny cracks) and shrinkage (reduction in volume) during curing and service [7]. These limitations restrict their large-scale use in structural applications, necessitating the development of reinforcement strategies to enhance toughness, ductility, and durability.

There is a variety of approaches that have been investigated in an attempt to address the fragility of geopolymers, that is, the incorporation of natural fibres. In fact, natural fibres are biopolymer composites composed mainly of a network of cellulose (40–60 wt%), hemicelluloses

*Corresponding author: mouna.sellami@fss.u-sfax.tn

(20–40 wt%), and lignin (10–25 wt%) [7]. Recently, increasing attention has been given to the incorporation of cellulose in construction materials [8-10], and optical devices [11, 12] and water treatment [13] with the aim of finding a solution to this issue, due to their low cost, renewability, and eco-friendliness.

The main objective of this study was to investigate the effect of natural cellulose derived from sugar cane on the properties of alkali-activated geopolymers. Structural evaluations and UV-VIS absorbance were investigated according to the amount of incorporated cellulose via XRD diffraction, morphology analysis, FTIR spectroscopy and optical analysis. The results of this study will improve our understanding of the effect of cellulose in natural fibre-reinforced geopolymers and will form the basis for further research and applications, particularly in the fields of optics and energy storage.

Materials and Methods

Raw material

The kaolin used in this work was collected in the locality of Tunisia. The clay powders were heated to 700°C for 5 hours to prepare a non-crystalline active metakaolin ($Al_2O_3 \cdot 2SiO_2$) as a precursor. Sodium hydroxide solution (8M) was prepared 24h before the synthesis of materials.

Additive

Sugarcane bagasse (150 g) was prehydrolyzed through treatment with HCl (1.5%; 1570.3 mL) for 2 h at 120°C in a 2 L stainless steel autoclave, electrically heated. The prehydrolyzed sugarcane bagasse was washed with water. After that, 100 g of prehydrolyzed sugarcane bagasse was treated with NaOH (20 g of NaOH in 300 mL water) at 170°C for 2 h, to produce pulp. The produced pulp had a brown, cotton-like shape, in contrast to the straw-like shape of sugarcane bagasse raw material. To remove lignin, the pulp (80 g) was bleached with $HClO_2$ (3%; 2.4 g in 4750 mL water) in the presence of acetic acid (1.7 mL) for 2 h at 80°C. During the reaction process, the pH increased to 10-12. Therefore, acetic acid was added to adjust the pH to 1–3 (acidic) to obtain pure α-cellulose.

Geopolymers preparation

Different cellulose contents (0.5 wt%, 1 wt%, 1.5 wt%, and 2 wt%) were mixed with a hydroxide solution (8M) until they were fully soluble. Metakaolin was then added to the mixture, with a liquid/solid ratio of 1, to produce geopolymer pastes. These pastes were stirred to remove air bubbles. Finally, they were cast into Teflon molds at an ambient temperature for 28 days.

Technical analysis

The first analytical technique employed was UV–Vis spectrometry. The UV–Vis spectra of the samples were recorded at various time intervals (1 h, 21 h, 48 h, 72 h, and 96 h) within the wavelength range of 300-700 nm using a UV–Vis Ultra 3660 spectrophotometer (Rigol Technologies Inc., Beijing, China).

X-ray diffraction (XRD) analyses were carried out using a Rigaku SmartLab diffractometer (Rigaku Corporation, Tokyo, Japan), operated under the following conditions: 45 kV voltage, 200 mA current, using CuKα radiation ($\lambda = 1.54059$ Å) and a parallel beam configuration ($2\theta/\theta$ scanning mode) over a 2θ range of 5–90°. The interpretation of diffractograms and the quantification of crystalline phases present in the synthesized materials were performed using the Rigaku Data Analysis PDXL 2 software (version 2.7.2.0) and the ICDD (International Center for Diffraction Data) database.

FTIR spectra of the materials were recorded using a Jasco FTIR 6300 spectrometer (Jasco Corporation, Tokyo, Japan), equipped with an attenuated total reflectance (ATR) accessory

featuring a diamond crystal and KRS5 lens. Measurements were carried out in the 400–4000 cm^{-1} spectral range, with a total of 30 scans per sample at a spectral resolution of 4 cm^{-1}.

Morphological and structural characterization of the synthesized materials was performed using scanning electron microscopy (SEM), with a Hitachi TM-4000plus II field-emission microscope equipped with an energy-dispersive X-ray spectrometer (EDX). This method enabled the investigation of particle size, surface morphology, and elemental composition. Operating parameters were adjusted according to the requirements of each investigation: the type of detector (secondary electrons – SE, backscattered electrons – BSE), accelerating voltage (5, 10, 15, or 20 kV), and magnification factor (x500 – x2500) were varied to obtain detailed images and data.

Results and Discussions

Structural characterizations

Fig.1. illustrates the phase identification of G_0, G_1 and G_2 by X-Ray diffraction analyses. The XRD diagrams of all geopolymers are characteristic of a semi-crystalline material typical of the amorphous aluminosilicate gel (N–A–S–H). The presence of a broad amorphous hump between ~20° and 40° confirms the geopolymer formation [3], [14].

The main crystalline phases identified in geopolymers are Quartz SiO_2 and illite, which are not reaction products, but rather residual phases inherited from the kaolin precursor. It indicated only a partial geopolymerization and the presence of unreacted particles in the geopolymers.

The characteristic diffraction peaks of illite were detected at 8.9°, 17.5°,19.7°,25.2° and 34.3°[15], accompanied by a slight shift on the $G_{0.5}$ diagram. This confirms that the kaolin used in this study is a mixture of kaolinite and illite. It is important to note that illite is a 2:1 clay mineral with limited geopolymerization activity [3], [16].

Minor crystalline phase corresponding to cellulose was detected and proven by the presence of sharp peaks at 22.6°,24° and 35.7°[14]. This proves that cellulose does not readily dissolve in an alkaline activator.

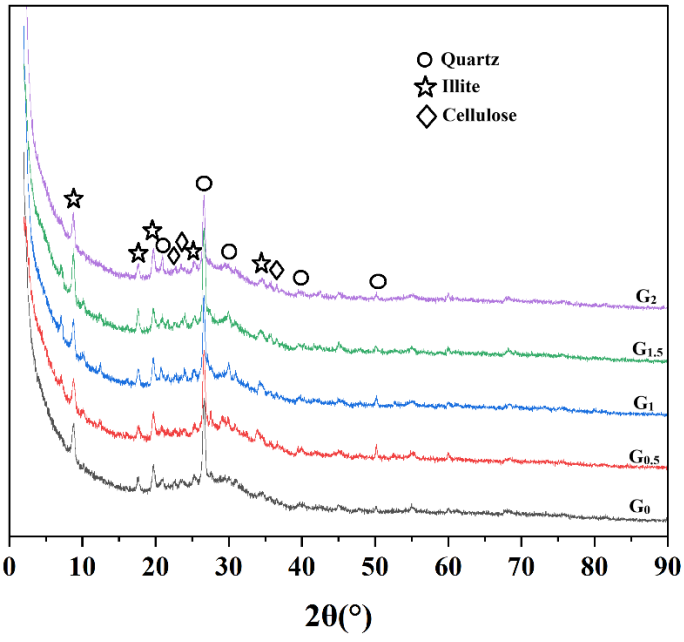

Fig. 1. XRD diagrams of geopolymers

SEM Analysis

Microstructural analysis of alkali-geopolymers was performed to gain a deeper understanding of the interaction between cellulose and the geopolymer gel. The SEM micrographs of the geopolymers matrix, with different magnification factors, are shown in Fig. 2.

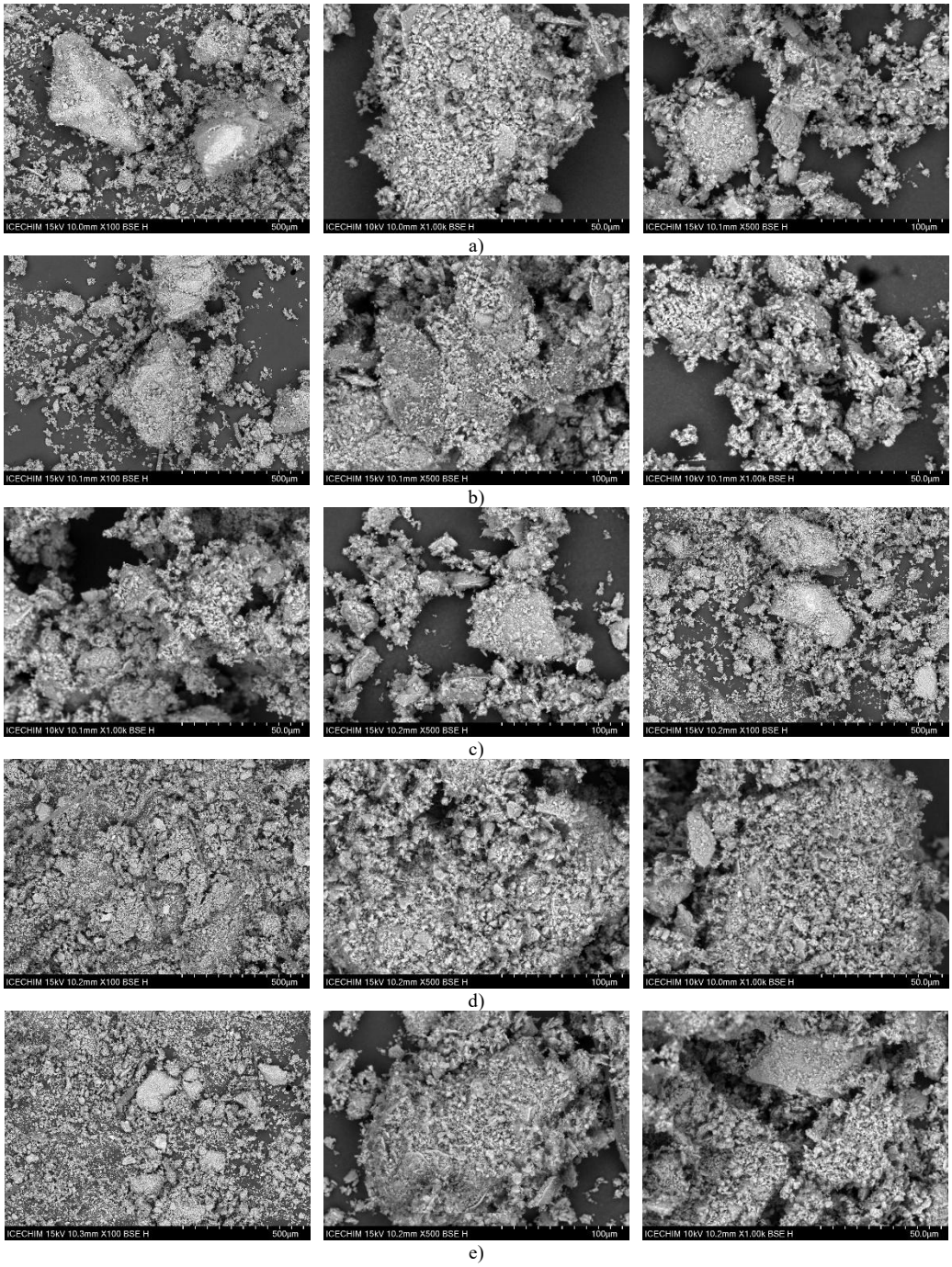

Fig. 2. SEM micrographs of: a) G_0; b) $G_{0.5}$; c) G_1; d) $G_{1.5}$ and G_2(e) with a magnification factor of (×100), (×500) and (×1000)

Fig 2. a) of pure geopolymer shows a relatively dense and continuous geopolymer matrix with some microcracks due to drying shrinkage. The matrix was heterogeneous with large unreacted particles. As cellulose content increases ($G_{0.5}$ to G_2), the geopolymer matrix becomes denser and more homogeneous.

As can be seen in Fig. 2(b) and (c), the addition of low cellulose content, 0.5% and 1%, respectively, affects fibre distribution, resulting in good dispersion. In contrast, the highest cellulose content (1.5% and 2%) leads to fibre agglomeration (Fig. 2 d) and e).

In addition, the insertion of cellulose leads to a successive increase in porosity, with the range extending from $G_{0.5}$ to G_2. It is common to see a noticeable increase in porosity when increasing cellulose content [17] . This occurs because fibres can trap air during mixing and create voids at the interface if the matrix paste is insufficient to fully coat each fibre (at high wt% of cellulose).

The microstructures indicate an optimal fibre content (between 0.5% and 1.5%) that maximizes benefits such as crack bridging and toughness without resulting in excessive porosity, which significantly weakens the composite. Based on the obtained results, sample (e), with a fibre content of 2%, represents a dosage beyond this optimum, at which point properties begin to degrade.

FTIR Spectroscopy

Fig.3. illustrates the FTIR spectra of all geopolymers to investigate the chemical bonds in their 3D networks. The FTIR spectra exhibit the typical vibrational modes of geopolymers, associated with O-H water bonds and Si–O–T (T = Si/Al) vibrational modes.

The wide vibration bands between 2960 and 3650 cm^{-1} and the sharp peak at around 1652 cm^{-1} exhibited in all spectra were attributed to O–H stretching and bending modes, respectively [18, 19].

The asymmetric stretching modes of Si–O-Al/Si links to the main peak in the 800-1200 cm^{-1} region, deconvoluted in two components centred at 870 and 956 cm^{-1} [10, 13].

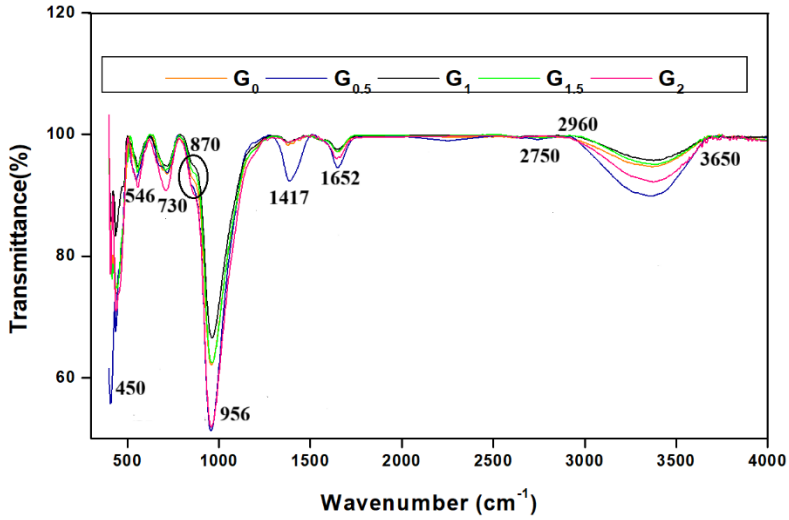

Fig. 3. FTIR spectra of geopolymer samples

The intensity of the peaks at 450 and 546 cm^{-1} was attributed to the Si-O bending vibration [19].

These band intensities increased when cellulose weight percentage was added, indicating the enhanced formation of C-A-S-H gels, consistent with the XRD results.

The small band around 730 cm^{-1} was caused by the symmetric stretching of Si-O-Si in quartz [20]. This finding corroborates the XRD patterns, which show the presence of the SiO_2 quartz phase.

In addition, the chemical composition of natural fibre observed in all geopolymer-based cellulose was represented in the peaks at 2750 cm^{-1} and 1417 cm^{-1}, corresponding to the C-H and C-O vibration mode, respectively [10], [21]. The $G_{0.5}$ spectrum displays the highest intensity of these bands.

The FTIR analysis revealed a structural impact on the alkali-geopolymer framework resulting from cellulose loading. Particularly, the organic fiber affects the broadening and the intensity of Si-O-T and Si-O bonds within the framework. This effect was not noticeable for the O-H, C-O, and C-H bonds, which were broader and intense on the $G_{0.5}$ spectrum.

This confirmed that cellulose has an influence on the geopolymerization process.

UV-VIS analysis

The effect of the natural fibre (cellulose) on the optical properties is described in Fig.4.

All samples exhibit a similar spectral shape. As shown, the sample with the highest cellulose content (G_2) presents a consistent increase in the baseline, as well as the highest absorbance across the entire measured range (from 280nm to 800nm), compared to other samples.

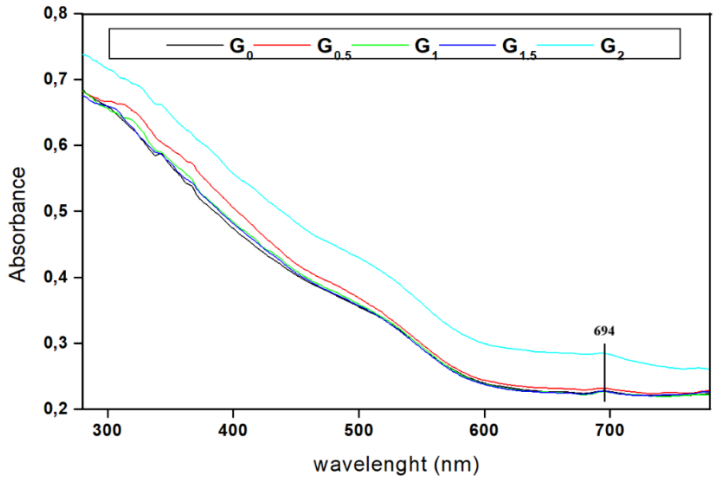

Fig. 4. UV-Visible absorption of geopolymer samples

This is probably due to a combination of increased diffuse scattering caused by cellulose fibres dispersed in the solid matrix and the formation of cellulose-derived conjugated chromophores in an alkaline environment [11].

In contrast, an increase in absorbance intensity at lower cellulose loadings suggests limited chemical modification at these wt%.

The presence of a sharp peak at around 694 nm in all spectra is likely due to an instrument problem or cellulose-derived conjugated chromophores phenomena [12].

Difference spectra ($G_2 - G_0$) reveal a broad, featureless contribution consistent with the additional light attenuation introduced by the incorporation of cellulose. This suggests that the incorporation of cellulose enhances the light absorbance, particularly in the UV range, indicating possible photocatalytic benefits.

The microstructural analysis of the samples demonstrated a positive effect of cellulose addition on the homogeneity and integrity of the matrix. In contrast, samples without natural fiber addition exhibited a high number of cracks and a heterogeneous structure. Those with cellulose addition, however, displayed a much more compact morphology and improved dissolution of the

raw materials. Additionally, FTIR and UV-VIS analyses confirmed the presence of the fibres as distinct compounds within the geopolymer structure. This indicates that the cellulose fibres did not fully dissolve during mixing and activation; instead, they partially retained their structure, contributing to the overall improvement of the geopolymer's properties.

Conclusions

The primary objective of the present work was to assess the impact of cellulose on the structural characteristics and optical properties of metakaolin-based geopolymers. A series of geopolymers was successfully synthesized via the activation of a hydroxide alkaline solution and metakaolin containing varying amounts of cellulose (0.5 wt%, 1 wt%, 1.5 wt%, and 2 wt%). The physicochemical properties of the geopolymers were examined by XRD, SEM, FTIR, and UV-VIS analyses.

To conclude, the addition of small amounts of cellulose (0.5 wt% and 1 wt%) improves the geopolymer microstructure, making it denser and more uniform. Additionally, a lower cellulose weight results in better incorporation of natural fibre into the geopolymer matrix.

However, higher cellulose content (1.5 wt% and 2 wt%) enhances porosity and heterogeneity, which could decrease mechanical performance in future applications, but might improve functional properties such as light absorption and the geopolymerization process.

Acknowledgments / Funding body

The authors are grateful to AUF for the award of a postdoctoral fellowship at the University of Sfax, and Faculty of Material Science and Engineering, Gheorghe Asachi Technical University of Iasi.

References

[1] J. Davidovits, *Geopolymers*, **Journal of Thermal Analysis**, **37(8)**, 1991, pp. 1633-1656, doi: 10.1007/BF01912193.

[2] M. Sellami, M. Barre, M. Toumi, *Synthesis, thermal properties and electrical conductivity of phosphoric acid-based geopolymer with metakaolin*, **Applied Clay Science**, **180**, 2019, p. 105192, doi: 10.1016/j.clay.2019.105192.

[3] M. Sellami, M. Barre, M. Toumi, *The New Challenge of Acid-Based Geopolymers Synthesized with the Incorporation of Lithium Ions as Cathode Materials for Lithium-Ion Batteries*, **J Inorg Organomet Polym**, 30(8), 2020, p. 3126-3131, 2020, doi: 10.1007/s10904-020-01475-z.

[4] L. Angelova, D.D. Burduhos-Nergis, A. Surleva, A.V. Sandu, D. Ilieva, G.E. Chernev, P. Vizureanu, *Study of Heavy Metal Encapsulation in Geopolymerized Industrial Waste by Sequential Extraction,* **JOM: the journal of the Minerals, Metals & Materials Society**, **77(3)**, 2024, doi: 10.1007/s11837-024-07049-5.

[5] Y. Xie, C. Wang, Y. Guo, H. Cui, J. Xue, *Improved mechanical and thermal properties of sustainable ultra-high performance geopolymer concrete with cellulose nanofibres*, **Journal of Building Engineering**, **102**, 2025, p. 112068, doi: 10.1016/j.jobe.2025.112068.

[6] C. Lv, J. Liu, G. Guo, Y. Zhang, *The Mechanical Properties of Plant Fiber-Reinforced Geopolymers: A Review*, **Polymers**, **14(19)**, 2022, p. 4134, doi: 10.3390/polym14194134.

[7] N. Ranjbar, M. Zhang, *Fiber-reinforced geopolymer composites: A review*, **Cement and Concrete Composites**, **107**, 2020, p. 103498, doi: 10.1016/j.cemconcomp.2019.103498.

[8] Y. Habibi, L. A. Lucia, O. J. Rojas, *Cellulose Nanocrystals: Chemistry, Self-Assembly, and Applications*, **Chem. Rev.**, **110(6)**, 2010, p. 3479-3500, doi: 10.1021/cr900339w.

[9] S. Rocha Ferreira, N. Ukrainczyk, K. Defáveri Do Carmo E Silva, L. Eduardo Silva, E. Koenders, *Effect of microcrystalline cellulose on geopolymer and Portland cement pastes mechanical performance*, **Construction and Building Materials**, **288**, 2021, p. 123053, doi: 10.1016/j.conbuildmat.2021.123053.

[10] Y. Xie, C. Wang, Y. Guo, H. Cui, J. Xue, *Improved mechanical and thermal properties of sustainable ultra-high performance geopolymer concrete with cellulose nanofibres*, **Journal of Building Engineering**, **102**, 2025, p. 112068, doi: 10.1016/j.jobe.2025.112068.

[11] F. Wang *al.*, *Functionalized Cellulose Derivatives: Challenge or Opportunity in the Field of Chiral and Achiral Sensing*, **Critical Reviews in Analytical Chemistry**, **1**, p. 1-18, doi: 10.1080/10408347.2025.2512176.

[12] N. H. M'sakni T. Alsufyani, *Part B: Improvement of the Optical Properties of Cellulose Nanocrystals Reinforced Thermoplastic Starch Bio-Composite Films by Ex Situ Incorporation of Green Silver Nanoparticles from Chaetomorpha linum*, **Polymers (Basel)**, **15(9)**, 2023, p. 2148, doi: 10.3390/polym15092148.

[13] L. Bertolla, G. Taveri, P. Mácová, K. Sotiriadis, F. Šiška, *Improving the cellulose/metakaolin geopolymer composite properties through a novel low-water approach,* **Materials letters**, **383**, 2025, p. 137967, doi: 10.1016/j.matlet.2024.137967.

[14] I. Kurek *al.*, *Foamed Eco-Geopolymer Modified by Perlite and Cellulose as a Construction Material for Energy-Efficient Buildings*, **Energies**, **15(12)**, 2022, p. 4297, doi: 10.3390/en15124297.

[15] S. Louati, S. Baklouti, B. Samet, *Acid based geopolymerization kinetics: Effect of clay particle size*, **Applied Clay Science**, **132-133**, 2016, p. 571-578, doi: 10.1016/j.clay.2016.08.007.

[16] *Geothermal Data Repository (GDR)*, **GDR**. Available online: https://gdr.openei.org/, retieved on 15 august 2025.

[17] I. Kurek *al.*, *Foamed Eco-Geopolymer Modified by Perlite and Cellulose as a Construction Material for Energy-Efficient Buildings*, **Energies**, **15(12)**, 2022, p. 4297, doi: 10.3390/en15124297.

[18] A. Gharzouni, L. Vidal, N. Essaidi, E. Joussein, S. Rossignol, *Recycling of geopolymer waste: Influence on geopolymer formation and mechanical properties*, **Materials & Design**, **94**, 2016, p. 221-229, doi: 10.1016/j.matdes.2016.01.043.

[19] H. Ye, Y. Zhang, Z. Yu, J. Mu, *Effects of cellulose, hemicellulose, and lignin on the morphology and mechanical properties of metakaolin-based geopolymer*, **Construction and Building Materials**, **173**, 2018, p. 10-16, doi: 10.1016/j.conbuildmat.2018.04.028.

[20] C. Wang, O. Kayali, J.-L. Liow, U. Troitzsch, *Participation and disturbance of superplasticisers in early-stage reaction of class F fly ash-based geopolymer*, **Construction and Building Materials**, **403**, 2023, p. 133176, doi: 10.1016/j.conbuildmat.2023.133176.

[21] N. Siti Syazwani, M. N. Ervina Efzan, C. K. Kok, M. J. Nurhidayatullaili, *"Analysis on extracted jute cellulose nanofibers by Fourier transform infrared and X-Ray diffraction"*, **Journal of Building Engineering**, **48**, 2022, p. 103744, doi: 10.1016/j.jobe.2021.103744.

Received: April 11, 2025
Accepted: June 28, 2025